Excitations in a 2D Metal-Insulator Array

B. G. Chen

Harvard College, Cambridge, Massachussetts 02138

D. Stroud

Department of Physics, The Ohio State University, Columbus, Ohio 43210-1106

(Dated: February 6, 2006)

Abstract

We write down the equations needed to calculate TE and TM waves propagating in a periodic array of cylindrical holes in a metal screen. The TE band structures are found to have one or two band gaps below the plasma frequency. The TM modes below the plasma frequency are found to be very flat, and there is some evidence of interaction with the free lattice band structure. The bottom of the TE band is found to be approximated well by a Wigner-Seitz type approximation.

I. INTRODUCTION

The field of photonics has recently concentrated on the behavior of EM waves in periodic dielectric and metallic structures. Following the lead of Yablonovitch[1], these systems have been studied to find gaps where EM modes with certain frequencies are forbidden. Many systems have been examined, including dielectric cylinders in a different dielectric[2], metallic cylinders in a dielectric[3–7], and even air cylinders in a superconducting composite[8].

In this paper, we consider a 2D system of air cylinders (holes) in a metal medium. Recent work on this type of system, however has focused on transmission through the grating parallel to the air cylinders[9]. We start section II by solving Maxwell's equations for our system, and then calculating the transverse modes of TE and TM waves traveling perpendicular to the holes by the plane-wave expansion method. When we apply this method to the E-polarized modes, we get a linear eigenvalue problem that we can solve numerically. However, when we use this method with the H-polarized modes, we get a nonlinear problem. If we use the technique of linearization, we can convert this to a linear problem.

In section III, motivated by the similarity of the equation for the E-polarized modes, we use an approximation based on a method of Wigner and Seitz[12] to find the position of the lowest band of the E-polarized modes.

In section IV, we show the band structures for different values of f, the ratio of the area of the hole to the area of the lattice cell, for both E and H polarized modes. We also show the agreement between the Wigner-Seitz approximation and the plane-wave method over a large range of f.

In section V, we discuss conclusions and possible future investigations.

II. FORMALISM

A. System under consideration

We consider a metal containing a 2D array of cylindrical holes, arranged in a square lattice. We take the holes to have radius a and we assume that they are separated by a distance d (fig. (1)). The metal is assumed to have a Drude dielectric constant (in SI units)

$$\frac{\epsilon(\omega)}{\epsilon_0} = 1 - \frac{\omega_p^2}{\omega^2}. \tag{1}$$
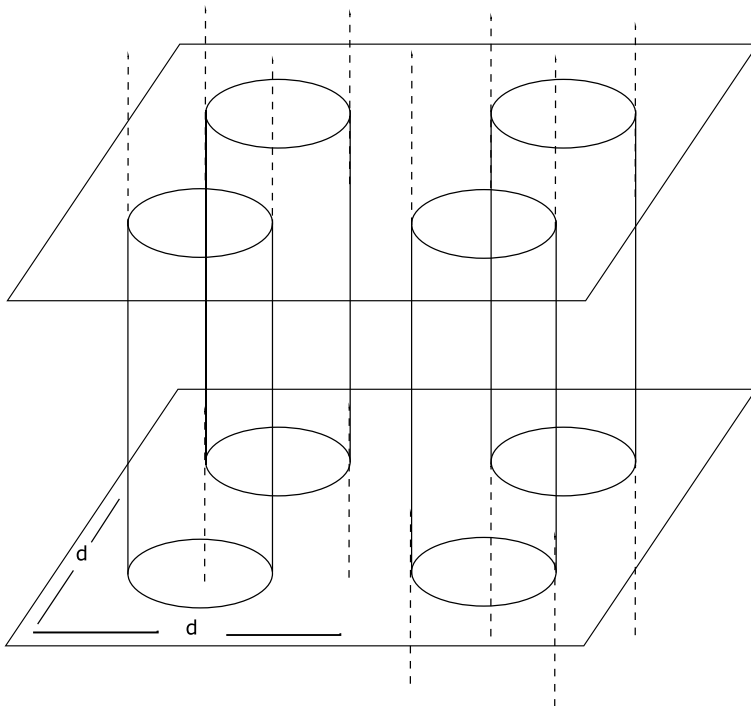
FIG. 1: The system consists of an array of cylindrical holes (we considered both square and circular cross sections) in an infinite metal medium.

Thus, we can write the position-dependent dielectric function of the screen as

$$\frac{\epsilon(\omega, \mathbf{x})}{\epsilon_0} = 1 - \frac{\omega_p^2 \theta(\mathbf{x})}{\omega^2}, \tag{2}$$

where we define $\theta(\mathbf{x})$ so that $\theta(\mathbf{x}) = \omega_p^2$ if the point $\mathbf{x} = (x, y)$ is within the metal, and $\theta(\mathbf{x}) = 0$ otherwise.

Now Maxwell's equations take the form (again in SI units)

$$\nabla \times \mathbf{E} = -\frac{\partial \mathbf{B}}{\partial t} \tag{3}$$

and

$$\nabla \times \mathbf{H} = +\frac{\partial \mathbf{D}}{\partial t}, \tag{4}$$

with $\nabla \cdot \mathbf{B} = 0$ and $\nabla \cdot \mathbf{D} = 0$.

Now we assume that all fields have an $e^{-i\omega t}$ time-dependence. Thus, in the above equations, we replace $\partial/\partial t$ by $-i\omega$. Also, we write $\mathbf{D}(\mathbf{x}, \omega) = \epsilon(\mathbf{x}, \omega)\mathbf{E}(\mathbf{x}, \omega)$. This gives

$$\nabla \times \mathbf{E}(\mathbf{x}, \omega) = i\omega \mathbf{B}(\mathbf{x}, \omega) \tag{5}$$

and

$$\nabla \times \mathbf{B}(\mathbf{x}, \omega) = -i\mu_0 \epsilon(\mathbf{x}, \omega)\omega \mathbf{E}(\mathbf{x}, \omega). \tag{6}$$

3

B.   Modes with $\mathbf{E} = E(\mathbf{x})\hat{z}$

If we take the curl of eq. (5) and substitute eq. (6) into the right-hand side, we obtain

$$\nabla \times \nabla \times \mathbf{E}(\mathbf{x}, \omega) = \omega^2 \mu_0 \epsilon(\mathbf{x}, \omega)\mathbf{E}. \tag{7}$$

Using the fact that $\mu_0 \epsilon_0 = 1/c^2$, where c is the speed of light in vacuum, we have

$$\nabla \times \nabla \times \mathbf{E} = \frac{\omega^2}{c^2}\left(1 - \frac{\omega_p^2 \theta(\mathbf{x})}{\omega^2}\right)\mathbf{E}. \tag{8}$$

We will now look for a special kind of solution to this wave equation, namely, one in which $\mathbf{E}(\mathbf{x}) = E(\mathbf{x})\hat{z}$. This is a transverse wave propagating in the xy-plane, but with $\mathbf{E}\|\hat{z}$. We can then turn the above equation into a scalar wave equation, by using the identity $\nabla \times \nabla \times \mathbf{E} = \nabla(\nabla \cdot \mathbf{E}) - \nabla^2\mathbf{E}$, and noting that $\nabla \cdot \mathbf{E} = 0$. The result is the following *scalar* wave equation for $E(\mathbf{x})$, the z-component (and only non-vanishing component) of the electric field:

$$\left(-\nabla^2 + \frac{\omega_p^2 \theta(\mathbf{x})}{c^2}\right)E(\mathbf{x}) = \frac{\omega^2}{c^2}E(\mathbf{x}). \tag{9}$$

Eq. (9) is identical in form to the 2D Schrödinger equation. The first term on the left is like the kinetic energy (with $\hbar^2/2m = 1$). The second term is like the potential energy: it vanishes inside the holes and is a constant between the holes. Finally, ω^2/c^2 plays the role of the energy eigenvalue. Therefore, in order to find the propagating modes, one needs to solve the Schrödinger equation in 2D for this type of potential.

Now, how does one calculate the states of this periodic potential? There are a number of ways to proceed. First of all, since the potential is periodic, we know that the "wave function" (the z-component of the electric field, in this case) has to satisfy Bloch's theorem, and must therefore be of the form

$$E(\mathbf{x}) = \exp(i\mathbf{k} \cdot \mathbf{x})u_{\mathbf{k}}(\mathbf{x}) \tag{10}$$

where $u_{\mathbf{k}}(\mathbf{x})$ is a periodic function of x and y with the period of the lattice, and $\mathbf{k} = (k_x, k_y)$ is a two-component wave vector.

One way to solve eq. (9) is to expand the solution in a Fourier series. For example, let us suppose that we are interested in a square lattice of holes, with lattice constant d. Then $u(\mathbf{x}) = u(\mathbf{x} + \mathbf{R})$ where $\mathbf{R} = n_1 d\hat{x} + n_1 d\hat{y}$, where n_1 and n_2 are integers. Hence, $u(\mathbf{x})$ can be expanded in a Fourier series of the form

$$u(\mathbf{x}) = u_{\mathbf{K}}e^{i\mathbf{K}\cdot\mathbf{x}} \tag{11}$$

4

where

$$\mathbf{K} = n_1 \frac{2\pi}{d} \hat{x} + n_2 \frac{2\pi}{d} \hat{y}. \tag{12}$$

Substituting eq. (11) into eq. (9), and noting that $\nabla^2 \exp(i(\mathbf{k} + \mathbf{K}) \cdot \mathbf{x}) = -|\mathbf{k} + \mathbf{K}|^2 \exp(i(\mathbf{k} + \mathbf{K}) \cdot \mathbf{x})$, we get

$$\sum_{\mathbf{K}} |\mathbf{k} + \mathbf{K}|^2 u_{\mathbf{K}} e^{i(\mathbf{k}+\mathbf{K}) \cdot \mathbf{x}} + \frac{\omega_p^2 \theta(\mathbf{x})}{c^2} \sum_{\mathbf{K}} u_{\mathbf{K}} e^{i(\mathbf{k}+\mathbf{K}) \cdot \mathbf{x}} = \frac{\omega^2}{c^2} \sum_{\mathbf{K}} u_{\mathbf{K}} e^{i(\mathbf{k}+\mathbf{K}) \cdot \mathbf{x}}. \tag{13}$$

Eq. (13) can be turned into a matrix equation by the following procedure. Left-multiply both sides by $e^{-i(\mathbf{k}+\mathbf{K}') \cdot \mathbf{x}}$, where $\mathbf{K}' = n_1'(2\pi/d)\hat{x} + n_2'(2\pi/d)\hat{y}$, and integrate over the "unit cell" $-d/2 < x < d/2$, $-d/2 < y < d/2$. The integral

$$\int_{-d/2}^{d/2} dx \int_{-d/2}^{d/2} dy e^{i(\mathbf{K}-\mathbf{K}') \cdot \mathbf{x}} = \delta_{\mathbf{K},\mathbf{K}'} \tag{14}$$

where $\delta_{a,b}$ is the Kronecker delta function, and $\delta_{\mathbf{K},\mathbf{K}'} = 1$ if $\mathbf{K} = \mathbf{K}'$ and 0 otherwise.

Thus, eq. (13) reduces to the following:

$$|\mathbf{k} + \mathbf{K}'|^2 u_{\mathbf{K}'} + \frac{\omega_p^2}{c^2} \sum_{\mathbf{K}} W_{\mathbf{K}-\mathbf{K}'} u_{\mathbf{K}} = \frac{\omega^2}{c^2} u_{\mathbf{K}'} \tag{15}$$

Here the Fourier component $W_{\mathbf{K}-\mathbf{K}'}$ is given by

$$W_{\mathbf{K}-\mathbf{K}'} = \frac{1}{d^2} \int_{-d/2}^{d/2} dx \int_{-d/2}^{d/2} dy e^{-i(\mathbf{K}'-\mathbf{K}) \cdot \mathbf{x}} \theta(\mathbf{x}) \tag{16}$$

Eq. (15) is a matrix equation for the Fourier components $u_{\mathbf{K}}$ of the "wave function" $E(\mathbf{x})$. Note that eq. (15) can be written formally as:

$$\left(\mathbf{R} - \frac{\omega^2}{c^2} \mathbf{I} \right) u_{\mathbf{K}} = 0 \tag{17}$$

where $\mathbf{R}$ is the matrix representation of the right hand side of eq. (15) as an operator on the matrix $u_{\mathbf{K}}$ and is a function of the Bloch vector $\mathbf{k}$. Note that this actually represents an infinite number of equations (one for each reciprocal lattice vector $\mathbf{K}$). Thus the problem of finding the bands is equivalent to solving the eigensystem shown here.

In the finite wave approximation, the bands can be approximated by cutting off the number of reciprocal lattice vectors $\mathbf{K}$ considered and then solving the resulting finite eigenvalue / eigenvector problem with any convenient program.

5

C.   Modes with $\mathbf{H} = H(\mathbf{x})\hat{z}$

Let us now try to find propagating solutions with $\mathbf{H} = H(\mathbf{x})\hat{z}$. Substituting this form into Maxwell's equations, we obtain

$$\nabla \times \left[\frac{1}{\epsilon} \nabla \times \mathbf{H} \right] = \frac{\omega^2}{c^2} \mathbf{H}. \tag{18}$$

Substituting the form $\mathbf{H} = H(\mathbf{x})\hat{z}$, we may rewrite this equation as

$$\nabla \cdot \left(-\frac{1}{\epsilon} \nabla H \right) + \frac{\omega^2}{c^2} H = 0. \tag{19}$$

For a periodic lattice, and with $\epsilon(\omega, \mathbf{x}) = 1 - \omega_p^2 \theta(\mathbf{x})/\omega^2$, this equation takes the form

$$\nabla \cdot \left[-\frac{1}{1 - \omega_p^2 \theta(\mathbf{x})/\omega^2} \nabla H \right] + \frac{\omega^2}{c^2} H = 0. \tag{20}$$

Then the differential equation becomes

$$\nabla \cdot \left\{ \left[\frac{1}{1 - \omega_p^2/\omega^2} \theta(\mathbf{x}) + 1 - \theta(\mathbf{x}) \right] \nabla H \right\} + \frac{\omega^2}{c^2} H = 0. \tag{21}$$

Multiplying by $\omega^2 - \omega_p^2$, we obtain

$$\nabla \cdot \left\{ \left[\omega^2 \theta(\mathbf{x}) + (\omega^2 - \omega_p^2)(1 - \theta(\mathbf{x})) \right] \nabla H \right\} + \frac{\omega^2(\omega^2 - \omega_p^2)}{c^2} H = 0, \tag{22}$$

which becomes

$$\nabla \cdot \left\{ \left[\omega^2 - \omega_p^2(1 - \theta(\mathbf{x})) \right] \nabla H \right\} + \frac{\omega^2(\omega^2 - \omega_p^2)}{c^2} H = 0. \tag{23}$$

We Fourier-expand the solution with

$$H(\mathbf{x}) = \sum_{\mathbf{K}} \mathbf{v_K} \exp(i(\mathbf{k} + \mathbf{K}) \cdot \mathbf{x}) \tag{24}$$

$$\theta(\mathbf{x}) = \sum_{\mathbf{K}'} W_{\mathbf{K}'} \exp(i\mathbf{K}' \cdot \mathbf{x}). \tag{25}$$

We left-multiply by $e^{-i(\mathbf{k}+\mathbf{K}+\mathbf{G})\cdot\mathbf{x}}$ where $\mathbf{G}$ is an arbitrary reciprocal lattice vector, then integrate over the unit cell, and group terms by powers of ω^2, and the result is:

$$\omega^4 \mathbf{v_G} - \omega^2(\omega_p^2 + c^2 ||\mathbf{k}+\mathbf{G}||^2)\mathbf{v_G} + \omega_p^2 \left(\mathbf{v_G} - c^2 \sum_{\mathbf{K}} [(\mathbf{k}+\mathbf{K}) \cdot (\mathbf{k}+\mathbf{G})W_{\mathbf{G}-\mathbf{K}}] \mathbf{v_K} \right) = 0 \tag{26}$$

Now, we rewrite eq. (26) as a polynomial with matrix coefficients:

$$\omega^4 \mathbf{I} + \omega^2 \mathbf{A} + \mathbf{B} = 0 \tag{27}$$

6

where $\mathbf{A}$,$\mathbf{B}$ are the matrix representations of the operators on $\mathbf{v_G}$, and $\mathbf{I}$ is the identity matrix.

This is a quadratic determinant equation for ω^2 and to solve with the finite wave approximation, we use the technique of linearization[5,10,11], used by Kuzmiak and Maradudin in calculating modes in the "inverse" of this system (i.e. metal cylinders in air)[5]. Let

$$\mathbf{v}^* = \begin{pmatrix} \omega^2\mathbf{v} \\ \mathbf{v} \end{pmatrix} \qquad (28)$$

Then solving this eigenvalue problem is equivalent to solving for the frequencies ω^2 in eq. (26), with the condition that the bottom half of the components of the eigenvectors correspond to the eigenvectors of eq. (26).

$$\begin{pmatrix} \mathbf{A} & \mathbf{B} \\ \mathbf{I} & 0 \end{pmatrix} \mathbf{v}^* = \omega^2\mathbf{v}^* \qquad (29)$$

This is a usual eigenvalue problem, and can be solved by computer as with the $\mathbf{E}$-polarized case.

D. Calculation of W for Square and Circular Cross-sectional holes

Let f be the hole area fraction, that is, the ratio of the area of the hole to the area of each lattice cell. Then the calculation of the Fourier coefficients $W_{\mathbf{K}}$ of the step function θ representing the hole for a square yields

$$W_{\mathbf{K}} = (1 - f)\delta_{\mathbf{K},\mathbf{0}}, \qquad (30)$$

and for a circle,

$$W_{\mathbf{K}} = \delta_{\mathbf{K},\mathbf{0}} - \frac{2\sqrt{\pi f}}{||\mathbf{K}||d}J_1\left(d||\mathbf{K}||\sqrt{\frac{f}{\pi}}\right), \qquad (31)$$

where $J_1(\cdot)$ is the first order Bessel function of the first kind. For the circular formula, we take $W_0 = 1 - f$, in accordance with its value in the limit of $\mathbf{K} \to \mathbf{0}$.

III. WIGNER-SEITZ APPROXIMATION TO CALCULATE FREQUENCY OF BOTTOM OF LOWEST BAND

The Wigner-Seitz approximation is a way of calculating the lowest energy eigenvalue of an electron in a periodic solid[12]. We adapt this approach to the present problem.

A.   E-polarization

The method is as follows: The lowest frequency eigenvalue occurs at the Γ point, i. e., at $\mathbf{k} = 0$. At that point, the "wave function" [i. e., the z-component of the electric field, which we have been calling simply $E(\mathbf{x})$] is periodic:

$$E(\mathbf{x} + \mathbf{R}) = E(\mathbf{x}), \tag{32}$$

where $\mathbf{R} = n_1 a\hat{x} + n_2 a\hat{y}$ is a lattice vector. Thus, right at the *boundary* of the square unit Wigner-Seitz cell (defined by $-a/2 < x < +a/2$, $-a/2 < y < +a/2$), the normal derivative of $E(\mathbf{x}) = 0$. Specifically, we claim that

$$\left(\frac{\partial E(\mathbf{x})}{\partial x}\right)_{x=\pm a/2} = 0, \tag{33}$$

and

$$\left(\frac{\partial E(\mathbf{x})}{\partial y}\right)_{y=\pm a/2} = 0. \tag{34}$$

Inside the unit cell, $E(\mathbf{x})$ satisfies

$$\left(-\nabla^2 + \frac{\omega_p^2}{c^2}\theta(\mathbf{x})\right) E(\mathbf{x}) = \frac{\omega^2}{c^2}E(\mathbf{x}). \tag{35}$$

This is a well-defined boundary value problem, but not so convenient to solve, because of the square boundary. In the Wigner-Seitz approximation, we simplify the problem by replacing the square by a *circle* of the same area. Therefore, the Wigner-Seitz approximation to our present boundary-value problem for $E(\mathbf{x})$ is

$$\left(-\nabla^2 + \frac{\omega_p^2}{c^2}\theta(\mathbf{x})\right) E(\mathbf{x}) = \frac{\omega^2}{c^2}E(\mathbf{x}) \tag{36}$$

for $r < R$, and

$$\left(\frac{\partial E}{\partial r}\right)_{r=R} = 0, \tag{37}$$

where $\pi R^2 = d^2$.

For the case of circular holes in a metallic screen, this equation becomes simpler, because the hole function $\theta(\mathbf{x})$ is only a function of $r = \sqrt{x^2 + y^2}$. Thus, we expect that the ground state is cylindrically symmetric: $E(\mathbf{x}) = E(r)$. We can write the Laplacian in polar coordinates as $\nabla^2 = (1/r)(\partial/\partial r)(r\partial/\partial r)$ (for a cylindrically symmetric function). Thus, the differential equation for $E(r)$ becomes

$$-\frac{1}{r}\frac{\partial}{\partial r}\left(r\frac{\partial E(r)}{\partial r}\right) + \frac{\omega_p^2}{c^2}\theta(r)E(r) = \frac{\omega^2}{c^2}E(r). \tag{38}$$

8

For the cylindrical holes, this problem is particularly easy to solve. We have $\theta(r) = 1$ for $r > a$ and $\theta(r) = 0$ for $r < a$, where $a = d\sqrt{\frac{4f}{\pi}}$ is the hole radius when d is the lattice constant and f is the hole area fraction. The equation then takes the form of a Helmholtz equation inside and outside the hole with different constants. The solutions take the form of linear combinations of zeroth order Bessel functions of the first and second kind (J_0 and Y_0). For $r < a$, the solution of the differential equation must only have a J_0 term because of the smoothness condition at $r = 0$. We also assume an arbitrary normalization such that

$$E(r) = J_0(kr), \tag{39}$$

where $k = \omega/c$. For $r > a$, the solution is a linear combination of both J_0 and Y_0 with coefficients A and B:

$$E(r) = AJ_0(k'r) + BY_0(k'r), \tag{40}$$

where $k' = \sqrt{\omega^2 - \omega_p^2}/c$.

The continuity, derivative continuity and vanishing normal derivative boundary conditions form a set of equations from which A and B can be eliminated, resulting in

$$k'J_0(ka)[J_1(k'R)Y_1(k'R) - J_1(k'a)Y_1(k'a)] = kJ_1(ka)[J_1(k'R)Y_0(k'a) - J_0(k'a)Y_1(k'R)]. \tag{41}$$

We can solve this transcendental equation for ω (in this form hidden in k and k') numerically and the lowest solution results in an approximation for the frequency of the lowest plasmon level.

B. H-polarization

In contrast to the linearity of the E-polarized equation, the equation for the H-polarized waves is highly nonlinear. We can expand the divergence in eq. (23) and we get

$$[\omega^2 - \omega_p^2(1 - \theta)]\nabla^2 H + \omega_p^2\nabla H \cdot \nabla\theta + \frac{\omega^2(\omega^2 - \omega_p^2)}{c^2}H = 0 \tag{42}$$

$$[\omega^2 - \omega_p^2(1 - \theta)]\nabla^2 H + \omega_p^2\delta(r - a)\nabla H \cdot \hat{r} + \frac{\omega^2(\omega^2 - \omega_p^2)}{c^2}H = 0 \tag{43}$$

Here a is the hole radius and $\delta(\cdot)$ is the Dirac delta function (not to be confused with the notation $\delta_{a,b}$ which represents the Kronecker delta).

In both the domains $r < a$ and $r > a$, the above equation simplifies to the Helmholtz equations describing the E-polarized waves. However, the boundary condition at the hole
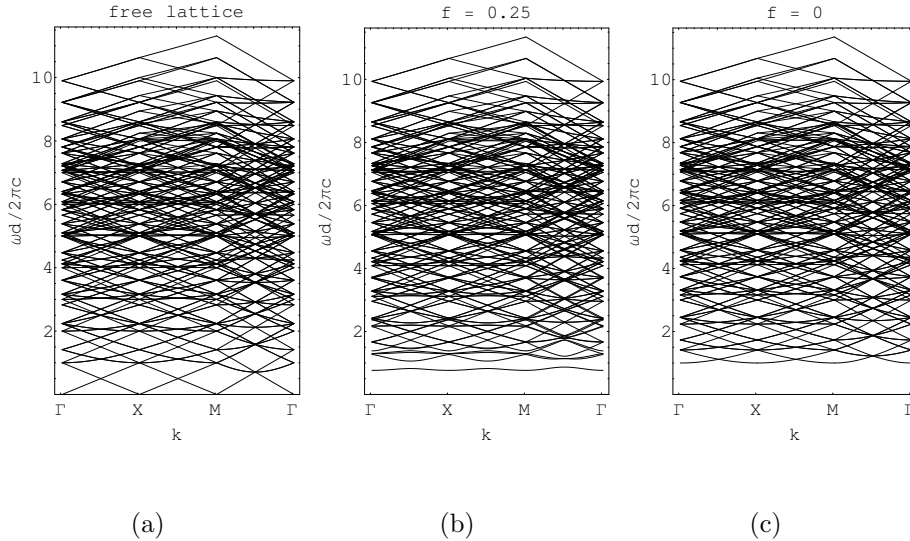
9

FIG. 2: The complete calculated photonic band structure of a square lattice of cylindrical holes in a metal system. E-polarized system. (a) Free lattice (no metal). (b) $f = .25$. (c) No hole ($f = 0$).

edge $r = a$ is no longer simple continuity, but rather, a difficult one involving a Dirac delta function. We have not yet attempted to calculate the corresponding Wigner-Seitz approximation for the H-polarization.

IV.   NUMERICAL RESULTS

All plane-wave expansion calculations used 225 plane waves, and $\omega_p d/2\pi c = 1$.

A.   E-polarization Band Structure

For the E-polarized waves, we found that approximately the bottom half of the bands were convergent with any given number of plane waves. When we added more plane waves, the new bands were added above the pattern established by the lower energy plane waves. Thus, we expect that the band structures for all systems extend to infinity.

Above approximately $\omega d/2\pi c = 2.5$, there is a somewhat periodic band structure (periodic with ω, see fig. 2 from $\omega d/2\pi c = 3$ to 4, 4 to 5, etc.) which is mostly invariant for all the E-polarized systems. We expect that the cutoff around $\omega d/2\pi c = 10$ is a numerical artifact, and the true band structure is an infinite number of copies of this structure, extending to
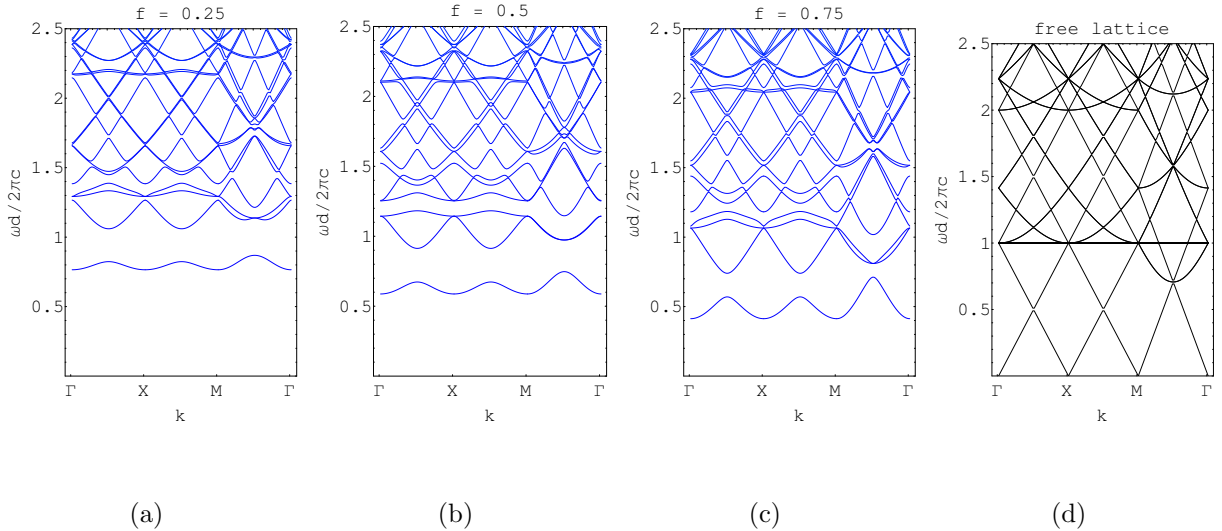
10

FIG. 3: The photonic band structure of a square lattice of cylindrical holes in a metal system. E-polarized system. (a) $f = .25$. (b) $f = .5$. (c) $f = .75$. (d) free lattice.

infinity.

If we consider only the bands below $\omega d/2\pi c = 2.5$ (fig. 3), we see that the lowest gap which decreases in size as f increases since the lowest band level is decreasing. For $f > 0$ there is a band below ω_p and a gap between this band and the next higher band which decreases as f increases also. When we reach the free lattice case, there no longer is a band gap, and the modes fill up all frequencies.

B.   H-polarization Band Structure

Because of the linearization technique, we had to diagonalize matrices which were twice as large as those of the E-polarized modes, thus 450×450 rather than 225×225, and likewise, we had twice as many bands. No matter how many plane waves we used, half the bands lay above ω_p and half lay between 0 and ω_p. Regarding the convergence of the bands above ω_p, since again there is a finite cutoff, we expect that the bands in this grouping closest to ω_p are converged. For the bands between 0 and ω_p, convergence was slower but also started from the bands closest to ω_p.

Above $\omega = \omega_p$, the H-polarized bands are qualitatively similar to the E-polarized bands (fig. 4), and as expected, when we calculate H-polarized modes in either the free lattice or
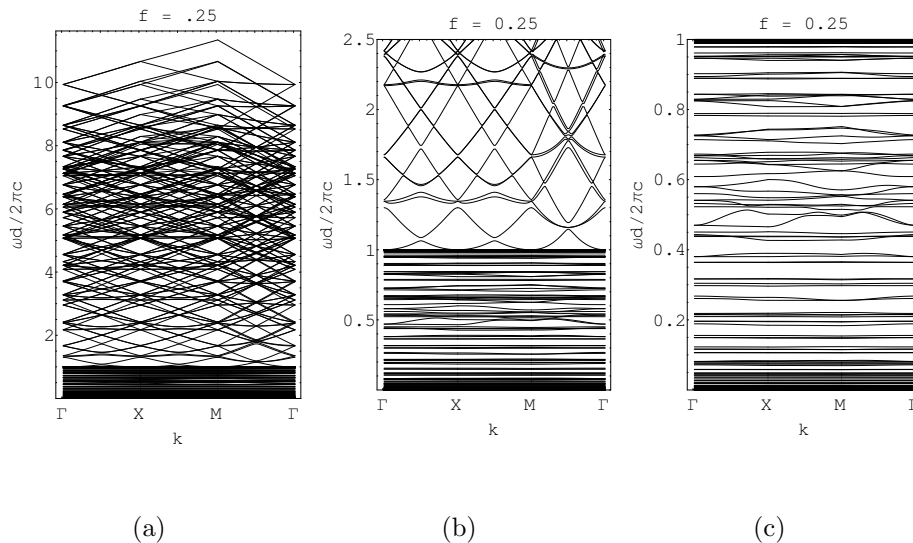
11

FIG. 4: The calculated photonic band structure of a square lattice of cylindrical holes in a metal system with $f = .25$. H-polarized system. (a) All bands shown. (b) Below $\omega d/2\pi c = 2.5$. (c) Below $\omega d/2\pi c = 1$.

the $f = 0$ (no hole) cases, they correspond exactly to what we calculated with E. This is because these systems are completely isotropic, and thus there will be no distinction between various polarizations of EM waves.

However, when $f > 0$, flat bands begin to appear from $\omega = 0$ up until a maximum level between 0 and ω_p. As f increases, this maximum level of flat bands reaches ω_p, and the flat bands appear to fill up the region $0 < \omega < \omega_p$.

We noticed that the lowest flat bands appear to have some interaction with a parabolic pattern (fig. 5(a-c)). As f increases, the parabolic pattern also grows in size. The pattern appears to approach the free lattice band structure (fig. 3(d)). We also noticed that the bands just below ω_p also appear to interact with another parabolic pattern which resembles the free lattice band structure just below ω_p (fig. 5(d)), although the amplitude appears to be smaller (this may be because they are more converged).

C. E-polarization Wigner-Seitz Approximation Comparison

We generated a plot of $\omega d/2\pi c$ vs f for the E-polarized modes, and upon comparison to the numerical solution of the Wigner-Seitz approximation (fig. 6), we found near-coincidence
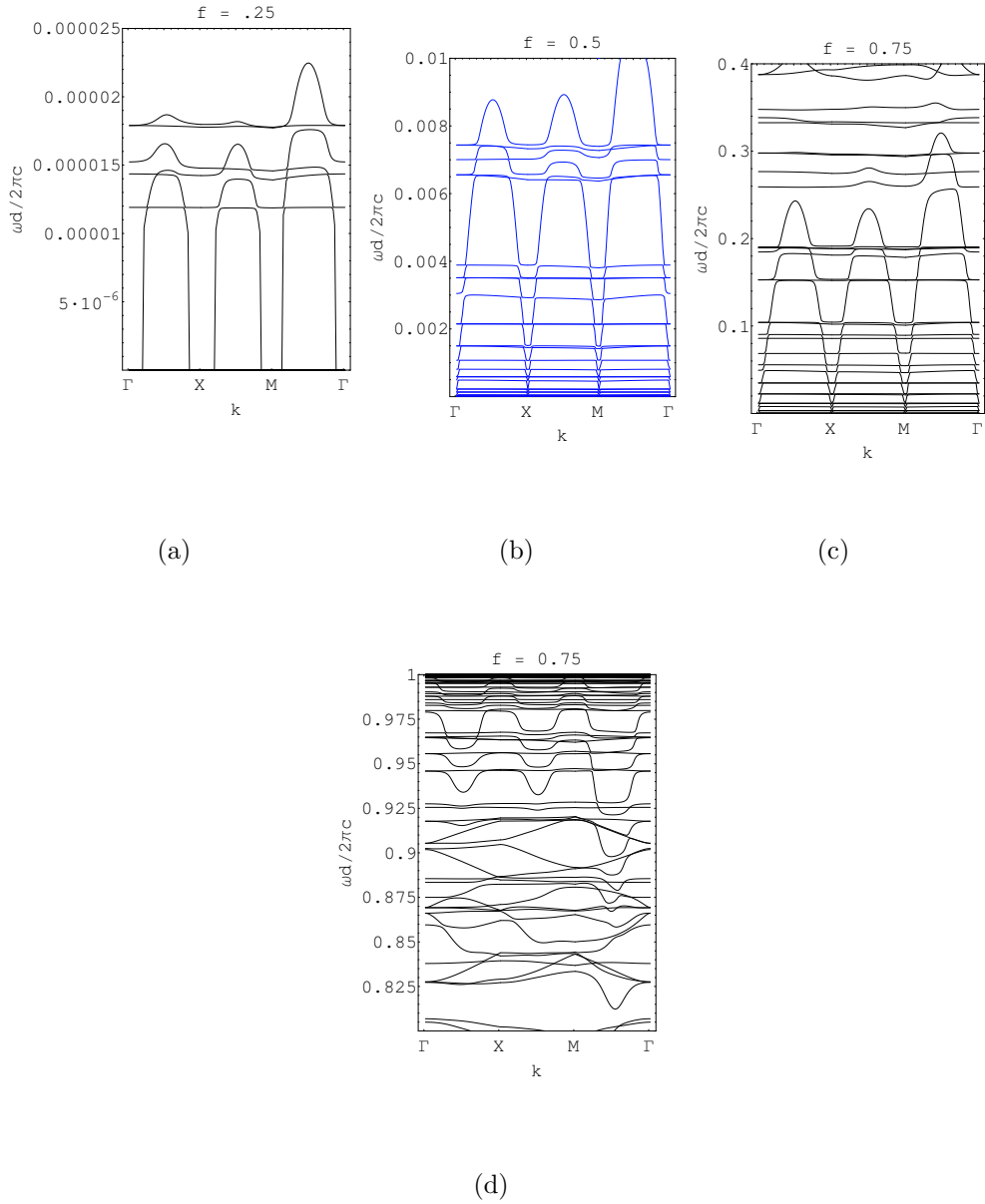
12

(a)

(b)

(c)

(d)

FIG. 5: The photonic band structure of a square lattice of cylindrical holes in a metal system. H-polarized system. (a) $f = .25$. (b) $f = .5$. (c) $f = .75$. (d) $f = .75$.

for values up to approximately $f = .45$, and values differing by less than 5% over the full range (up until $f = \pi/4$ which is the largest circular hole which fits in a single square lattice cell). Agreement at low f is expected because with a smaller hole size, the boundary conditions at the edge of the lattice cell (which are different for the two approaches) will have less effect on the mode than the condition at the edges of the hole (which are identical).

13

TABLE I: Comparison of E-polarization and W-S approx.

f	$\omega d/2\pi c$ (finite wave)	$\omega d/2\pi c$ (W-S)	% difference
0	1	1	0
.1	.9125	.9131	.06%
.2	.8101	.8118	.2%
.3	.7244	.7274	.4%
.4	.6523	.6571	.7%
.5	.5874	.5947	1%
.6	.5235	.5349	2%
.7	.4536	.4722	4%

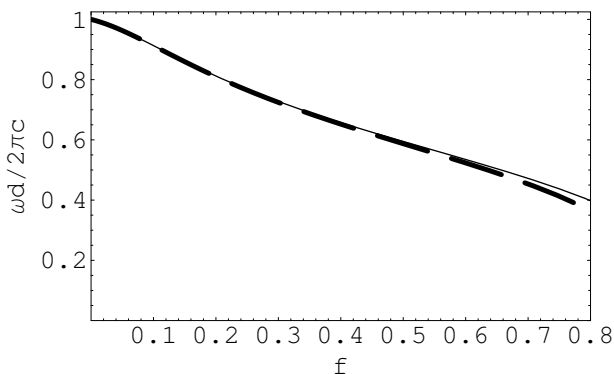FIG. 6: Position of lowest band of E-polarized waves vs f from the plane-wave expansion calculation (dashed) and the Wigner-Seitz approximation (solid).

V.   DISCUSSION AND CONCLUSIONS

We found in section IV that E-polarized waves with $f > 0$ have at least one band below the plasma frequency. This makes sense because the frequencies of the modes are intermediate between the free lattice (no band gap) and the metal medium without holes (no bands below ω_p). This behavior has been observed in other systems with metal components[3–5,7], with roughly the same ratio of metal to air, suggesting that qualitatively, the only important factor may be f, rather than the particular distribution of metal and air. Calculations with square holes rather than circular suggest this also.

For the H-polarized modes, the flat bands have been found by Kuzmiak and Maradudin

14

and others[5–7] in the system of metal cylinders in air - and the interaction with a perturbed free-space dispersion relation was noted in these papers also. In particular, Kuzmiak et. al[6] have suggested that the flat bands may be due to interaction with single-cylinder modes. The similarity of the behavior of metal cylinders in air to air cylinders in metal suggests that the qualitative behavior of EM waves is mostly determined by the relative amounts of metal and air in a system. The dependence on the geometry of the system rather than just the ratio of metal to air should be investigated also to see what geometrical features are most important.

We have not seen any other applications of this Wigner-Seitz approximation on photonic band structure calculations. Future work on this subject may be on investigating the behavior of the other roots of the transcendental equation (41) and their goodness of fit to the other bands of the E-polarized modes. Also, the behavior at points in the first Brillouin zone other than Γ should be characterized. Finally, it should be determined whether it is possible to extend this technique to H-polarized waves.

VI. ACKNOWLEDGEMENTS

[1] E. Yablonovitch, Phys. Rev. Lett. 58, 2059 (1987).

[2] W. Zhang, A. Hu, X. Lei, N. Xu, and N. Ming, Phys. Rev. B 54, 10280 (1996).

[3] M. Plihal, A. Shambrook, A. A. Maradudin, and P. Sheng, Opt. Commun. 50, 199 (1991).

[4] M. Plihal and A. A. Maradudin, Phys. Rev. B 44, 8565 (1991).

[5] V. Kuzmiak and A. A. Maradudin, Phys. Rev. B 55, 7427 (1997).

[6] V. Kuzmiak, A. A. Maradudin, and F. Pincemin, Phys. Rev. B 50, 16835 (1994).

[7] A. R. McGurn and A. A. Maradudin, Phys. Rev. B 48, 17576 (1993).

[8] W. M. Lee, P. M. Hui, and D. Stroud, Phys. Rev. B 51, 8634 (1995).

[9] T. W. Ebbesen, H. J. Lezec, H. F. Ghaemi, T. Thio, and P. Wolff, Nature 391, 667 (1998).

[10] G. Peters and J. H. Wilkinson, SIAM J. Num. Anal. 7, 479 (1970).

[11] S. Amari, R. Vahldieck, J. Borenmann, and P. Leuchtmann, IEEE Trans. Microwave Theory Tech. 48, 453 (2000).

[12] E. Wigner and F. Seitz, Phys. Rev. 44, 804 (1933).